

# INITIALIZATION EFFECTS VIA NUCLEAR CHARGE RADII PARAMETERIZATIONS ON THE NUCLEAR STOPPING AND ITS RELATION TO DISTRIBUTION AND PRODUCTION OF LIGHT MASS FRAGMENTS\*

SANGEETA

School of Physics and Materials Science, Thapar University  
Patiala 147004, Punjab, India

*(Received December 28, 2015)*

We present the initialization effects on the global stopping parameters and their correlation to the fragment production via different nuclear charge radii parameterizations using isospin-dependent Quantum Molecular Dynamics model at  $E = 50$  MeV/nucleon. The results obtained for liquid drop model (LDM) proposed nuclear charge radii parameterization which is isospin-independent — they have been compared with the results of three isospin-dependent nuclear charge radii parameterizations. We conclude that the values of global stopping parameters  $R$  and  $\frac{1}{Q_{zz}/\text{nucleon}}$  decrease with the increase in nuclear charge radii, while the production of fragments is reported to be enhanced. The influence of nuclear charge radii on nuclear stopping is almost the same for central and semi-central collisions. In addition, we have studied the role of isospin-dependent nuclear charge radii parameterizations on the  $N/Z$  dependence of global stopping parameters.

DOI:10.5506/APhysPolB.47.991

## 1. Introduction

One of the most fascinating topics of heavy ion collisions (HICs) are the structural effects on the nuclear reaction dynamics and its by-products. The low-energy nuclear dynamics is used to extract information regarding the nuclear structure which includes the properties such as shapes, deformations, size, *etc.* and fundamental research of important processes of nuclear fusion-fission. The HICs at intermediate energies are supportive to create highly dense, thermally excited and compressed nuclear matter state which depends on various entrance channel conditions. The extensive study of

---

\* Presented at the XXXIV Mazurian Lakes Conference on Physics, Piaski, Poland, September 6–13, 2015.

nuclear reactions with different neutron-to-proton ratios is contributive to essence the nuclear equation of state (NEOS) and the isospin physics for isospin asymmetric nuclear matter. In literature, the nuclear stopping is proved to be a good probe to study the NEOS and the role of isospin-dependent in-medium nucleon–nucleon ( $N$ – $N$ ) cross section, different kinds of symmetry potential and momentum-dependent interactions (MDI) [1–5]. From numerous observables of intermediate energy HICs, the study of nuclear stopping provides the information about the fragmentation phase transition and thermalisation as well as expansion of the system [1]. The isospin physics has been explored through various isospin-dependent quantities in HICs at intermediate energies.

In view of this, Yang and co-workers [2] studied the isospin effects of nuclear stopping observable through isospin dependence of  $N$ – $N$  cross section as well as symmetry energy and observed that at low-energy regime, nuclear stopping is sensitive to both isospin-dependent  $N$ – $N$  cross section and symmetry potential, whereas as the incident energy increases above Fermi energy, the impact of isospin-dependent  $N$ – $N$  cross section is more pronounced compared to symmetry potential. However, in Ref. [3], the momentum quadrupole and transverse-longitudinal ratio of momentum are found to be sensitive towards the isospin dependence of in-medium correction of two-body cross section. A weaker dependence of global nuclear stopping on initial  $N/Z$  ratio of colliding nuclei as well as on symmetry potential has been reported. Recently, Puri and collaborators [4] investigated the nuclear stopping and its relation to the origin of light charged fragments with isospin-dependent Quantum Molecular Dynamics (IQMD) model [6]. Their systematic study reported that the magnitude of nuclear stopping depends strongly on isospin-dependent  $N$ – $N$  cross section and weakly on symmetry energy. Moreover, Vinayak *et al.* [5] observed that the dependence of nuclear stopping on the different forms of density-dependent symmetry energy is very weak.

Another quantity which has been used to account for the isospin physics is the isospin-dependent nuclear charge radius. In the past few decades, the theoretical [7] as well as experimental [8] low-energy nuclear dynamics proposed the isospin dependence of nuclear charge radii parameterizations [which are based on many calculations like the deformation effects in the nucleus and isopin parameter ( $I = (N - Z)/A$ )]. These different parameterizations have been proved to be a good probe to embellish the isospin physics on collective flow [9] and multifragmentation [10] in HICs at intermediate energies. In this article, our aim is to study the initialization effects as well as isospin physics via different nuclear charge radii parameterizations (*i.e.* isospin-independent [11] and isospin-dependent [7] with additional isospin parameter term in  $A^{1/3}$  dependence of nuclear charge radii) on the nuclear stopping of isospin asymmetric reactions by means of IQMD model.

## 2. Results and discussion

Simulations are carried out for central and semi-central isospin asymmetric nuclear reactions of  $^{50}_{20}\text{Ca} + ^{50}_{20}\text{Ca}$ ,  $^{90}_{36}\text{Kr} + ^{90}_{36}\text{Kr}$ ,  $^{100}_{40}\text{Zr} + ^{100}_{40}\text{Zr}$ ,  $^{124}_{50}\text{Sn} + ^{124}_{50}\text{Sn}$ ,  $^{150}_{60}\text{Nd} + ^{150}_{60}\text{Nd}$  and  $^{197}_{79}\text{Au} + ^{197}_{79}\text{Au}$  ( $N/Z = 1.5$ ) at  $E = 50$  MeV/nucleon, using IQMD model with isospin-dependent  $N$ - $N$  cross section reduced by 10%, *i.e.*  $\sigma = 0.9 \sigma_{nn}^{\text{free}}$  along with linear density-dependent symmetry energy and soft equation of state [12]. Here, the nucleons are primarily initialized in a sphere of radius in accordance with the liquid drop model (LDM) [11], *i.e.*  $R_{\text{LDM}} = 1.12 A^{1/3}$ . To study the influence of isospin-dependent nuclear charge radii on nuclear stopping, we have included the three different parameterized forms of nuclear charge radii, *i.e.*  $R_{\text{NGO}}$ ,  $R_{\text{PP}}$  and  $R_{\text{RR}}$  [7]. One can refer to Ref. [10] for the details of these radii. Fermi momentum associated with the nucleons has been kept constant *i.e.* 268 MeV/ $c$  in the model. To describe the nuclear stopping, the observables used are quadrupole of single particle momentum distribution  $\langle Q_{ZZ} \rangle$ , defined as

$$\langle Q_{ZZ} \rangle = \sum_i^{A_{\text{tot}}} (2p_z^2(i) - p_x^2(i) - p_y^2(i)) , \quad (1)$$

and anisotropy ratio  $\langle R \rangle$ , defined as

$$\langle R \rangle = \frac{2 \left[ \sum_i^{A_{\text{tot}}} |p_{\perp}(i)| \right]}{\pi \left[ \sum_i^{A_{\text{tot}}} |p_{\parallel}(i)| \right]} . \quad (2)$$

Here, the composite mass number of the system ( $A_{\text{tot}}$ ) is the sum of the mass number of the projectile ( $A_{\text{P}}$ ) and target ( $A_{\text{T}}$ ) nuclei *i.e.*  $A_{\text{tot}} = A_{\text{P}} + A_{\text{T}}$ . The transverse and longitudinal momentum of the  $i^{\text{th}}$  particle are  $p_{\perp}(i) = \sqrt{p_x^2(i) + p_y^2(i)}$  and  $p_{\parallel}(i) = p_z(i)$ , respectively. For complete nuclear stopping, one can expect a single Gaussian shape of rapidity distribution of particles and the values of  $\langle R \rangle$  and  $\langle Q_{ZZ} \rangle$  are 1 and 0, respectively. In the present analysis, we have studied “inverse of  $\langle Q_{ZZ} \rangle$ ” because  $\langle R \rangle$  and  $\langle Q_{ZZ} \rangle$  behave in opposite fashion. Left panels of Fig. 1 show the influence of nuclear charge radii on the rapidity distribution of light mass fragments (LMFs) [ $2 \leq A \leq 4$ ] for central collisions of  $^{50}_{20}\text{Ca} + ^{50}_{20}\text{Ca}$  (lighter) and  $^{197}_{79}\text{Au} + ^{197}_{79}\text{Au}$  (heavier), respectively. The central panels [(c) and (d)] and right panels [(e) and (f)] represent the influence of nuclear charge radii on the system size dependence of  $\langle R \rangle$  and  $\langle \frac{1}{Q_{ZZ}/\text{nucleon}} \rangle$ , respectively, at scaled impact parameter of  $\hat{b} = b/b_{\text{max}} = 0.0$  (upper panel) and 0.5 (lower panel). Here,  $b_{\text{max}} = (R_{\text{P}} + R_{\text{T}})$  fm,  $R_{\text{P}}$  and  $R_{\text{T}}$  are the radii of target and projectile

nuclei. From Fig. 1, it has been observed that for lighter system, more particles are distributed near target and projectile rapidities, which results in a broader Gaussian shape as compared to heavier system. Moreover, a narrow Gaussian shape of distribution of particles indicates a better thermalization compared to a broader Gaussian shape. Therefore, with the increase in system mass, due to an increase in density and temperature, more thermalization is achieved and accordingly, nuclear stopping increases. This observation supports the observation of Ref. [2]. The findings of Ref. [10] elucidate that due to different nuclear charge radii parameterizations, the calculated radius of a particular nucleus increases as  $R_{\text{LDM}} < R_{\text{NGO}} < R_{\text{PP}} < R_{\text{RR}}$ .

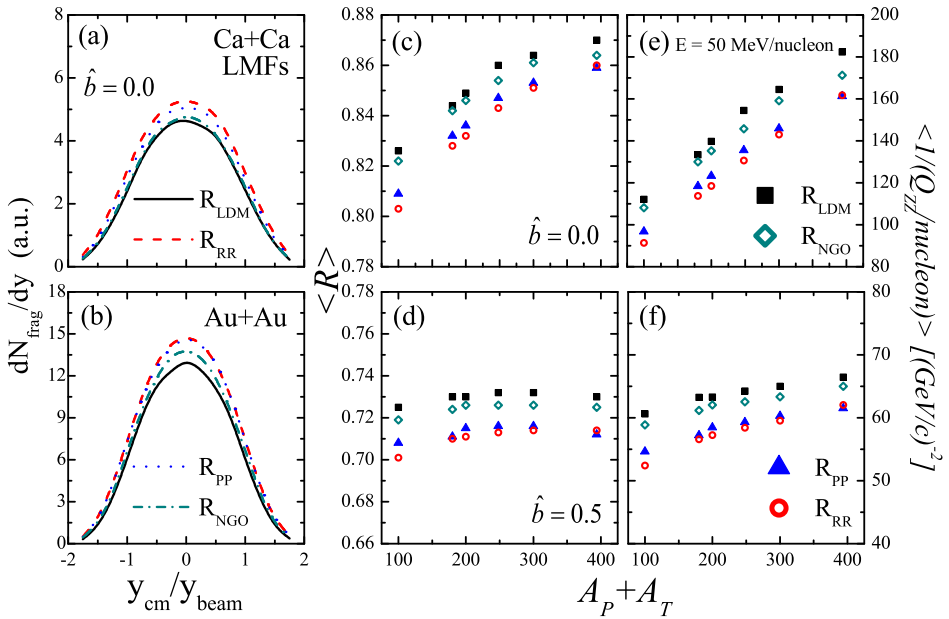


Fig. 1. Panels (a) and (b) display the rapidity distribution of LMFs for central Ca + Ca and Au + Au collisions, respectively, at  $E = 50$  MeV/nucleon. Panels (c) and (d) represent  $\langle R \rangle$ , whereas (e) and (f) represent  $\langle 1/(Q_{ZZ}/\text{nucleon}) \rangle$  as a function of system mass in central (upper panels) and semi-central (lower panels) collisions at  $E = 50$  MeV/nucleon.

Figure 1 reveals that the larger nuclear radii result in enhancement of production of LMFs which is due to the increase in the number of binary collisions. It has been noted that the system mass dependence of nuclear stopping observable in Fig. 1 of present work and multiplicity of LMFs in Fig. 3 of Ref. [10] follows the same trend which is in agreement with the findings of Ref. [4]; however, due to the increase in radius, the multiplicity

of fragments increases, but in the present scenario, we observe reduction in the nuclear stopping. This is because the increment in radius intensifies the transverse and longitudinal momentum of nucleons, which enhances the multiplicity of fragments. Whereas the probability of transformation of initial longitudinal momentum into transverse momentum is less with the larger radii. The increase in radius due to different isospin-dependent nuclear charge radii parameterizations causes the transformation of the longitudinal motion into transverse direction which consequently affects the degree of thermalization of the system. In other words, one can say that the percentage increment in the longitudinal momentum is higher compared to the transverse momentum, due to which nuclear stopping decreases. The percentage increment in radius is 12% for  $^{50}_{20}\text{Ca}$  and 8% for  $^{197}_{79}\text{Au}$  nuclei, corresponding to this change in radius, for central collisions, the value of  $\langle R \rangle$  (or  $\langle \frac{1}{Q_{zz}/\text{nucleon}} \rangle$ ) changes by 3% (or 18%) for  $\text{Ca} + \text{Ca}$  and 1.1% (or 11%) for  $\text{Au} + \text{Au}$  when switching from  $R_{\text{LDM}}$  to  $R_{\text{RR}}$ . Also, the dependence of nuclear stopping on system mass diminishes as the participant matter goes on reducing with the increase in colliding geometry, while the initialization effects via nuclear charge radii on nuclear stopping remain the same for central and semi-central collisions. Further, to observe the isospin effects on the  $N/Z$  dependence of nuclear stopping, we simulated the isobaric series of reactions of  $^{80}_{z_1}\text{X} + ^{80}_{z_1}\text{X}$  (where  $z_1 = 30, 32, 34, 36, 37, 38$  and  $40$ ) for semi-central collisions at  $E = 50$  MeV/nucleon displayed in Fig. 2. Referring to Fig. 5 of Ref. [10], we observe that the  $N/Z$  dependence of multiplicity of fragments is slightly affected by including isospin-dependent nuclear charge radii, whereas the behavior of nuclear stopping is independent towards  $N/Z$  content of colliding partners even if one considers isospin-dependent nuclear charge radii parameterizations.

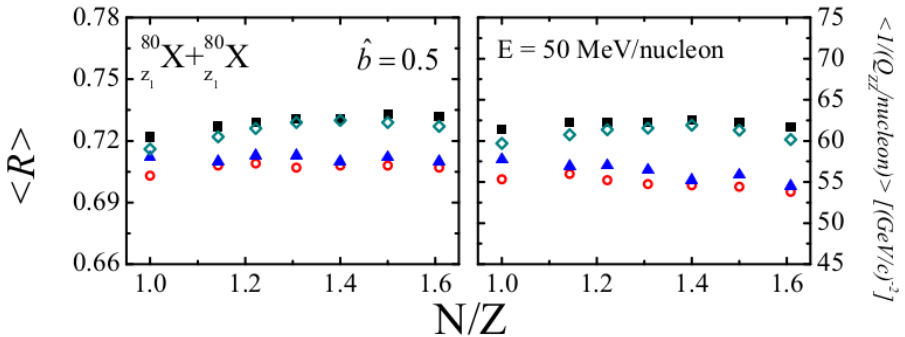


Fig. 2. Nuclear stopping observable  $\langle R \rangle$  (left panel) and  $\langle 1/(Q_{zz}/\text{nucleon}) \rangle$  (right panel) as a function of neutron-to-proton ratio in semi-central collisions of isobaric reactions with total mass 160 units at  $E = 50$  MeV/nucleon. Symbols have the same meaning as in Fig. 1.

### 3. Conclusion

In summary, we conclude that the increase in available phase space at initial state (due to different nuclear charge radii parameterizations) enhances the longitudinal as well as transverse momentum, which increases the production of fragments. However, the longitudinal momentum dominates the transverse momentum which, in turn, reduces the nuclear stopping. A ratio of change in the values of nuclear stopping to the change in radius is higher for lighter colliding nuclei pair compared to heavier one. The isospin-dependent nuclear charge radii are unable to alter the dependence of nuclear stopping on the initial neutron-to-proton content of the colliding nuclei for semi-central collisions at  $E = 50$  MeV/nucleon.

The financial support from the Department of Science and Technology (DST), Government of India in terms of INSPIRE-Fellowship (grant No. DST/INSPIRE/03/2014/000234) is gratefully acknowledged.

### REFERENCES

- [1] W. Bauer, *Phys. Rev. Lett.* **61**, 2534 (1988); F. Fu *et al.*, *Phys. Lett. B* **666**, 359 (2008).
- [2] Y.F. Yang *et al.*, *Chin. Phys. Lett.* **18**, 1040 (2001); J.Y. Liu *et al.*, *Phys. Rev. Lett.* **86**, 975 (2001).
- [3] Q.F. Li, Z.X. Li, *Chin. Phys. Lett.* **19**, 321 (2002).
- [4] J.K. Dhawan *et al.*, *Phys. Rev. C* **74**, 057901 (2006); S. Kumar, S. Kumar, R.K. Puri, *Phys. Rev. C* **81**, 014601 (2010).
- [5] K.S. Vinayak, S. Kumar, *J. Phys. G: Nucl. Part. Phys.* **39**, 095105 (2012).
- [6] C. Hartnack *et al.*, *Eur. Phys. J. A* **1**, 151 (1998); C. Hartnack *et al.*, *Phys. Rep.* **510**, 119 (2012).
- [7] H. Ngô, Ch. Ngô, *Nucl. Phys. A* **348**, 140 (1980); B. Nerlo-Pomorska, K. Pomorski, *Z. Phys. A* **344**, 359 (1993); **348**, 169 (1994); G. Royer, R. Rousseau, *Eur. Phys. J. A* **42**, 541 (2009).
- [8] I. Angeli, *At. Data Nucl. Data Tables* **87**, 185 (2004); I. Angeli, K.P. Marinova, *At. Data Nucl. Data Tables* **99**, 69 (2013).
- [9] R. Bansal, S. Gautam, R.K. Puri, J. Aichelin, *Phys. Rev. C* **87**, 061602(R) (2013); S. Gautam, *Phys. Rev. C* **88**, 057603 (2013).
- [10] Sangeeta, A. Jain, S. Kumar, *Nucl. Phys. A* **927**, 220 (2014).
- [11] A. Bohr, B. Mottelson, *Nuclear Structure*, W.A. Benjamin Inc., New York, Amsterdam, Vol. I, p. 268 (1969).
- [12] C. Hartnack, H. Oeschler, J. Aichelin, *Phys. Rev. Lett.* **96**, 012302 (2006).